Research Article Vol. 29, No. 11 / 24 May 2021 / Optics Express 17077
Optics EXPRESS

Widely tunable, low linewidth, and high power laser source using an electro-optic comb and injection-locked slave laser array

J. Connor Skehan, Corentin Naveau, Jochen Schroder, and Peter Andrekson*

Photonics Laboratory, Department of Microtechnology and Nanoscience, Chalmers University of Technology, SE - 412 96 Gothenburg, Sweden
Peter.Andrekson@Chalmers.SE

Abstract: We propose and implement a tunable, high power and narrow linewidth laser source based on a series of highly coherent tones from an electro-optic frequency comb and a set of 3 DFB slave lasers. We experimentally demonstrate approximately 1.25 THz (10 nm) of tuning within the C-Band centered at 192.9 THz (1555 nm). The output power is approximately 100 mW (20 dBm), with a side band suppression ratio greater than 55 dB and a linewidth below 400 Hz across the full range of tunability. This approach is scalable and may be extended to cover a significantly broader optical spectral range.

1. Introduction

A single-line, highly tunable, low linewidth, and high power source is highly desirable for applications such as spectroscopy, interferometry, and metrology [1–4], as well in communications [5–9]. They may also find uses as optical tweezers [10], for the detection of gravitational waves [11], and more.

Approaches to achieve this end range from semiconductor distributed feedback lasers (DFB) [12–15] and distributed Bragg reflector (DBR) lasers [16–20], to fiber-based ring lasers [1,21–26]. While these single frequency devices may produce high power and a low linewidth, unfortunately, their tunability is typically low, on the order of a few nanometers. On the other hand, frequency combs operate on a fixed grid and their power is distributed among many lines, which means that the OSNR of each tone after amplification is typically very low.

To overcome these limitation, we have implemented a system based on a commercial high coherence fiber laser, an electro-optic (EO) frequency comb, and an array of 3 commercially available DFB slave lasers which are used for injection locking of individual comb teeth. The result is a single frequency output which is tunable over nearly 1.25 THz within the C-Band (~10 nm), with approximately 100 mW of power, a side band suppression ratio of more than 55 dB, and less than 400 Hz of linewidth over the source's full range of tunability.

The underlying principle of the system begins with a low linewidth master laser which is modulated to produce cascaded, equally spaced side-bands. These comb lines inherit the optical properties of the source laser, but gain some additional phase noise due to the modulation. This results in the derived spectral linewidth of each tone increasing linearly as a function of the tone's modulation index, N. A single tone is then selected using a programmable optical filter (POF) and used for optical injection locking (OIL), a process in which a slave laser's emission is seeded by the injected optical field and overcomes the cavity's own spontaneous emission to induce lasing in accordance with the input optical field. The result is that the slave laser's output ideally follows the phase and frequency of the input field.

Since the frequency spacing of the EO comb's teeth is equal to the RF driving frequency, then, so long as the source laser is tunable over an optical bandwidth at least equal to the RF driving

#423794 https://doi.org/10.1364/OE.423794
Journal © 2021 Received 4 Mar 2021; revised 16 Apr 2021; accepted 17 Apr 2021; published 19 May 2021

Optics EXPRESS

frequency, the full comb can be shifted to overlap any desired frequency within its bandwidth by red or blue shifting the source frequency. Moreover, since the source laser's tuning range is greater than the frequency spacing of the EO comb, the achievable range may be extended by shifting the full comb beyond its overlap limit. To further increase the achievable frequency range, the approach may be upscaled via the use of additional slave lasers and the use of a broader comb source.

2. Experimental details

The principle of operation is seen in Fig. 1(A), an NKT Koheras fiber laser is used to produce an electro-optic frequency comb, after which a tone is selected using a programmable optical filter and used as the master field for injection locking one of a set of subsequent Gooch and Housego high power DFB slave laser. For simplicity, and to focus on principle of operation, several required optical components are omitted from Fig. 1(A), such as the polarization controllers required to align the injected field to the slave laser's active layer, splitters which are used to monitor power, etc.

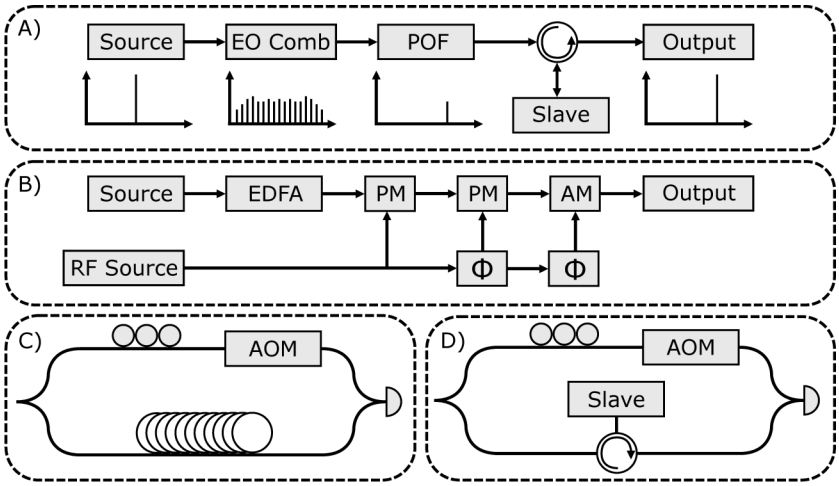

Fig. 1. A) The principle of operation, where a source is modulated to produce an EO Comb, a tone is then selected using a programmable optical filter, and a slave laser is injection locked to the selected tone. B) The generation of the optical frequency comb, using a fiber laser as the source, an erbium doped fiber amplifier (EDFA), two phase modulators (PM), one amplitude modulator (AM), some RF tone (in this case, a VCO), and two phase shifters. C) A delay line interferometer. D) A master-slave interferometer.

For instance, as seen in Fig. 1(B), the comb is created by injecting the source laser into an erbium doped fiber amplifier (EDFA) with a noise figure of approximately 4 dB for amplification up to 30 dB, and subsequently into a series of phase modulators (PM) which modulate the source to produce cascaded side-bands [27–32]. These side-bands are equally spaced from each other in accordance with the driving frequency, and inherit the noise properties of the seed laser and the RF source which modulates them. The breadth and shape of the produced optical spectra is represented mathematically as a summation of Bessel functions of the 1st kind [27].

$$\tilde{A}(\omega) = A_0 \sum_{N=-\infty}^{+\infty} J_n(KV_0) e^{iN\phi} \delta(\omega - N\omega_m - \omega_c) \tag{1}$$

Here, A is the amplitude, J_n are Bessel functions of the 1st kind which act as the envelop function which defines a comb of frequencies $\omega = N\omega_m + \omega_c$ where N is the comb tooth index, ω_m is the

Optics EXPRESS

modulation frequency, ω_c is the carrier frequency, K is the modulation index, V_0 is the amplitude of the modulating signal, and ϕ is the static phase noise induced by the voltage feed.

Importantly, the induced phase noise from the driving voltage grows linearly with tooth index, N, as per the $e^{iN\phi}$ term in Eq. (1). This corresponds to a linear increase in linewidth as the absolute tooth index increases, at a rate which depends on the phase noise of the RF source.

Next, this series of equally spaced frequency tones is injected into an Mach-Zehnder amplitude modulator (AM) which flattens the spectra. Note that the AM is not strictly necessary and could be omitted to extend the tuning range. However, its presence eases the characterization, hence we employed it in this setup.

When the phase offset between the driving tones of the PMs and AMs is correctly aligned, the result is a broad, flat-top EO comb which is sent into a programmable optical filter with a spectral width of 10 GHz. This filter selects individual teeth from the comb, either to have their linewidth measured or to act as a master for a subsequent slave laser.

Figure 1(C) shows the linewidth measurement system, which is based on the interference of two partially coherent beams. The detection method uses an optimized fiber length of 2.7 km, and electronically measures the peak and trough of the first interference peak, as well as the frequency spacing to the first interference peak. From these data points, we can estimate the linewidth of the laser with high accuracy, as has been previously demonstrated both theoretically and experimentally [33,34]. We refer the reader to [33] for a detailed analysis of the method used here. Our length of fiber delay line and choice of detector corresponds to an integration of the phase noise from 75 kHz (as determined by the fiber delay line length) up to 125 MHz (the receiver bandwidth). In all cases when measuring the linewidth, we keep the electrical spectrum analyzer's resolution bandwidth fixed at 200 Hz, and the video bandwidth fixed at 1 Hz. It's worth noting that the side lobe procedure used here assumes a white frequency noise laser source, and that the minimum measurable linewidth is set by the intersection of the 1/f noise influence and the noise floor influence on the measurement. In our case, the laser's phase noise is still frequency dependent over the integration bandwidths, and the minimum detectable linewidth occurs at approximately 220 Hz for the central tone.

Figure 1(D) shows a master-slave interferometer. Here, the source is split in two, one arm of which has its polarization modified to maximize interference with the opposite arm, and is frequency offset using an acousto-optic modulator (AOM) to offset frequencies from base-band, while the other arm passes through a circulator and into the slave laser, which in this case is a DFB laser without any optical isolator. By interfering the two beams on a photodiode and measuring the electrical output, we can verify that the slave laser cavity is locked to the master.

Figure 2 shows the fiber laser's optical spectra as measured on an optical spectrum analyzer (OSA) and its linewidth as measured using the linewidth characterization system described earlier, over its full thermally tunable frequency range. We can tune over a 115 GHz bandwidth, which corresponds to approximately 0.95 nm. The OSNR stays nearly constant at approximately 55 dB (with 0.1 nm resolution). The linewidth varies between approximately 200 Hz and 250 Hz over the tuning range. The double sided black arrow and dashed lines correspond to the frequency of RF modulation (25 GHz), and therefore the FSR of the EO Comb. Since the fiber laser's tunability is at least equal to the free spectral range (FSR) of the EO comb, the output can be tune to any frequency within the comb bandwidth by tuning the source laser and selection the appropriate comb line. Moreover, because the source tunability is greater than the frequency spacing of the comb (25 GHz), an additional 90 GHz of tunable range is added to the system via tuning the source past the comb's FSR.

Figure 3 shows a typical EO comb as created via modulation of the fiber laser, as well a comb envelope simulated using Eq. (1), the available tuning frequency of the fiber laser the DFB slave lasers (also seen in Table 1), and the power limit of stable injection locking. Here, the PM AM phase offsets of the comb are optimized for a balance of bandwidth and flatness, and the DFB

Optics EXPRESS

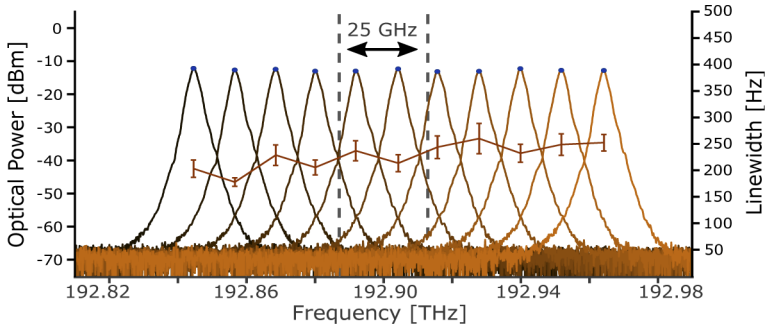

Fig. 2. The optical spectrum of the source fiber laser over its full range of thermal tunability, as well as the linewidth measured at each frequency. Optical spectra were measured with an OSA directly after the source with a resolution of 0.1 nm, and linewidth measurements were taken as described in the main text. The double sided arrow and dashed lines indicates a 25 GHz wide band, corresponding to the frequency of RF modulation used for comb creation. No amplification is present, and approximately 15 dB of loss is incurred before measurement.

slave lasers are tuned via a change in temperature. In general, for the injected beam to overcome the amplified spontaneous emission (ASE) and seed the lasing process [35,36] to induce optical injection locking, a variety of conditions must be met, related to the ratio of power in to fixed output power, linewidth enhancement factor of the cavity, and cavity quality factor [37,38]. The power of each tone in the comb is typically quite low resulting in limited use in real applications. While e.g. an EDFA can be certainly used to reach a desired power, the OSNR will then be (potentially unacceptably) low. In contrast, OIL acts simultaneously as an extremely narrowband optical filter and amplifier, which is therefore useful when amplifying light with a very narrow spectrum, such as the CW waves used here. Here, we fix all variables except the input power to the cavity which we allow to change, and find that at approximately −30 dBm of power, the injection locking is stable over a period of multiple days in the laboratory setting.

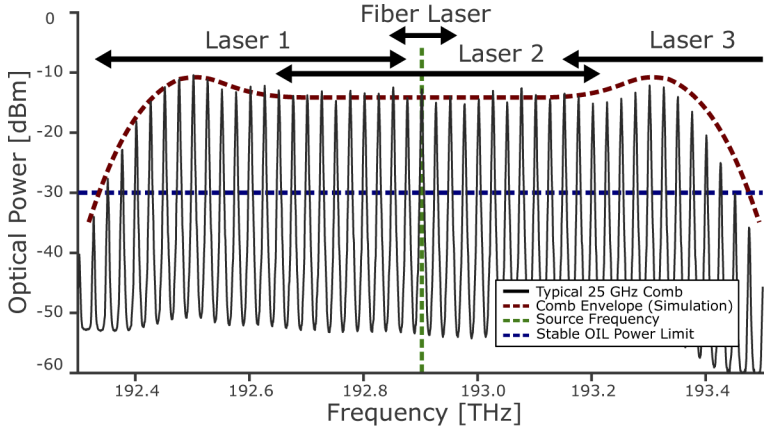

Fig. 3. A typical 25 GHz EO frequency comb as produced using the method described above in Fig. 1. Measurements were taken with an OSA tap directly after comb creation and with a resolution of 0.1 nm. Also indicated is a theoretical spectral envelope as produced via simulation using a noiseless RF clock at 25 GHz, $\frac{V}{V_\pi} = 10$, and with the central driving frequency of the fiber laser source at 192.9 THz, the stable injection locking limit of −30 dBm, the fiber laser tunability as seen in Fig. 2, and the available lasing frequencies for the array of DFB slave lasers, whose exact limits are seen in Table 1.

Optics EXPRESS

Table 1. The available temperature tuning of each slave laser in the DFB laser array.

	Min. Frequency	Max. Frequency	Frequency Range
Laser 1	192.330 THz	192.875 THz	0.545 THz
Laser 2	192.645 THz	193.215 THz	0.570 THz
Laser 3	193.150 THz	193.710 THz	0.560 THz

3. Results and discussion

As seen in Fig. 4, we begin by fully characterizing the linewidths of each unlocked comb tone as a function of frequency and for two different types of RF modulation. In Fig. 4(A), a small and relatively inexpensive voltage controlled osillator (VCO) is used, and in Fig. 4(B) a bulky, but tunable low-noise RF synthesizer is used. All measurements were taken 15 times with a minimum of −23.5 dBm on the photodiode to stay outside of the power-limited regime, and in all cases the $N = 0$ tone consistently approaches a linewidth value near 275 Hz.

Two full sets of measurements were taken using a commercial VCO, and an absolute value function is fit to the recovered data. On the first day we find a linewidth growth of approximately 606.1 Hz/THz, and two days later we find a linewidth growth of approximately 604.6 Hz/THz. Both values are within the error of fitting. Alternatively, this can be approximated as a linewidth growth of approximately 15 Hz/N. The data corresponding to the first day of operation is seen in Fig. 4(A).

Figure 4(B) depicts similar data which corresponds to identical conditions except for a change in RF clock. Here, instead of using a commercial VCO, we use a commercial low-noise RF synthesizer. Predictably, the phase noise is lower, and therefore the linewidth increase as a function of N is reduced. On the first day of measurement when using the RF synthesizer, and for a 25 GHz comb, we found a linewidth growth of approximately 181.9 Hz/THz. Two days later we find a value of 190.1 Hz/THz. Alternatively, this may be represented as a growth of approximately 4.5 Hz/N. Data from the first day is pictured.

Next, as shown in Fig. 5(A), we individually lock every tone of the 25 GHz EO comb after modulation with the RF synthesizer, and measure the linewidth of the injection locked slave laser output for each N tone. As before, the central tone at 192.9 THz approaches 275 Hz, and the rate of linewidth broadening is 168.2 Hz/THz, or approximately 4.5 Hz/N, which is similar to the previously measured value in the unlocked case. In general we observe no significant degradation of linewidth between the unlocked comb teeth in Fig. 4(B) and its individually injection-locked tones as seen in Fig. 5(A), indicating that OIL does not add to the linewidth growth rate as a function of N. Of note, the output power of the injection locked spectra is approximately invariant to input power and input frequency, and is fixed at approximately 20 dBm (100 mW) across the full breadth of the comb. This corresponds to a typical gain of 50 dB.

In Fig. 5(B), we see the output spectrum of the injection locked $N = 20$ tone as the central $N = 0$ tone (the source laser) is tuned from approximately 192.95 THz to 192.85 THz, as measured on the OSA at 0.01 nm resolution. For all injection locked tones measured, the output power is nearly constant at approximately 20 dBm (100 mW), and the side band suppression ratio is greater than 55 dB. Of note, the original linewidth of the unlocked slave lasers was on the order of a few hundred kHz, while the measured linewidths after injection locking are on the order of a few hundred Hz. We did not notice any change in the output spectrum between the locked and unlocked state of the DFB lasers at this OSA resolution, indicating that there was little to no degradation of the slave laser's spectrum caused by e.g. ASE from the pre-comb EDFA in the injection locking process.

Figure 6, shows the measured linewidth of 4 characteristic tones as a function of injection power. At −30 dBm of power, injection locking is stable over a period of multiple days with no

Optics EXPRESS

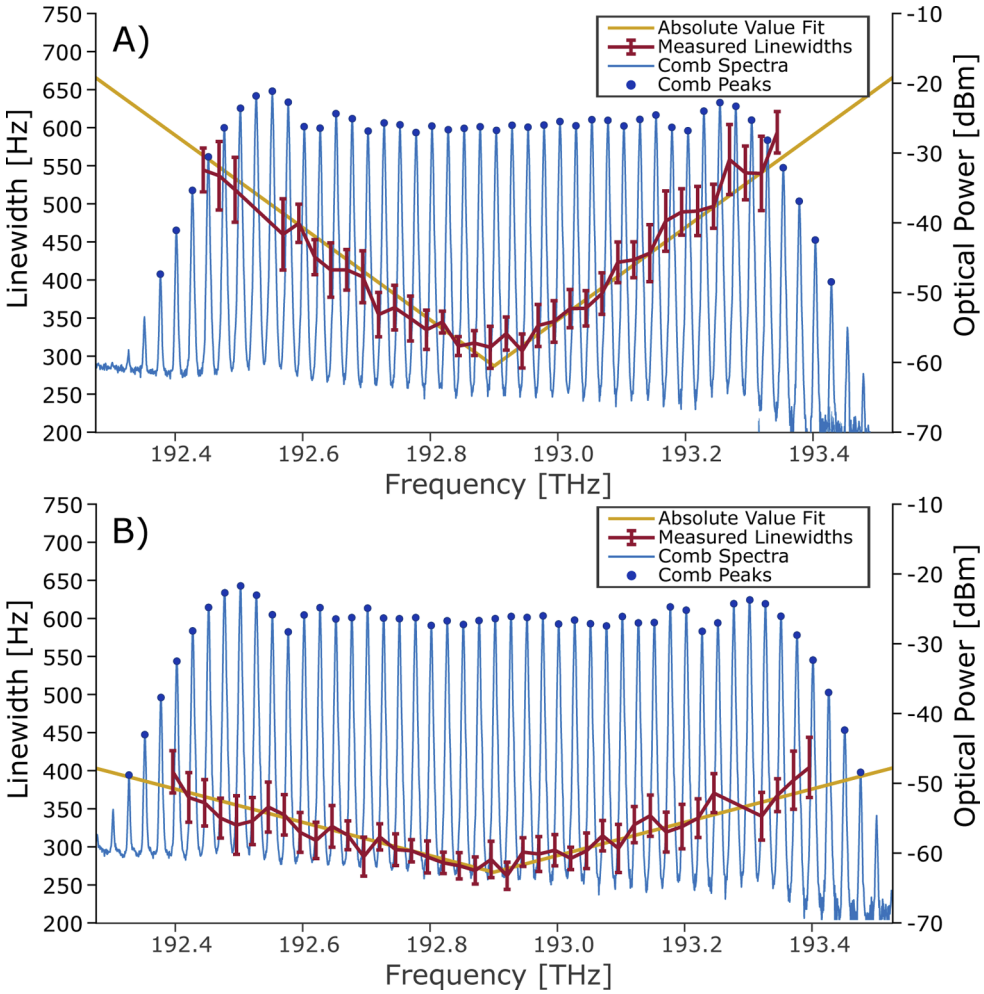

Fig. 4. A) Characterization of the unlocked 25 GHz EO comb when modulated using a commercial VCO B) A Characterization of the unlocked 25 GHz EO Comb when modulated using a commercial low-noise RF synthesizer. In all cases, 15 measurements were taken at each frequency, and the error bars represent the standard deviation of these measurements.

Optics EXPRESS

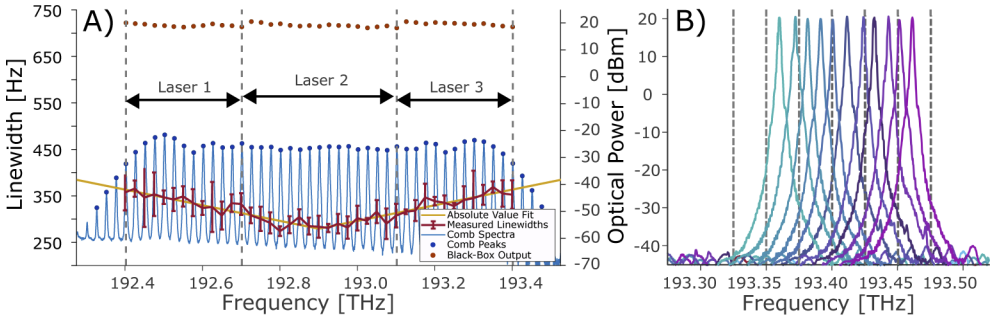

Fig. 5. A) Here, each tone of the EO comb has been injection locked to one laser in the DFB array, with the source fiber laser for EO comb creation at 192.9 THz. Here, all tones with a frequency less than 192.7 THz are locked to Laser 1, all tones above 193.1 THz are locked to Laser 3, and any intermediate tones are locked to Laser 2. In all cases, 15 measurements are taken at each frequency, and the error bars represent the standard deviation of these measurements. Tones below 192.4 THz and above 193.4 THz were not measured due to the instability of injection locking. For all tones, the injection locked power remains nearly constant across the full spectrum, and 20 dBm (100 mW) of power. B) The output spectrum of the injection locked slave laser, as measured using an OSA at 0.01 nm resolution, after tuning the source fiber laser from 192.95 THz to 192.85 THz, in increments of approximately 10 GHz. Dashed lines indicate 25 GHz increments.

required feedback loops. Below this level, injection locking is only stable over a period of a few hours, and below −40 dBm of input power, staying locked for a period of more than five minutes proved difficult. This "slipping out of lock" is what causes the increase in measured linewidth at low power. That said, no significant change in linewidth is observed when locked using between −40 and −12.5 dBm of input power.

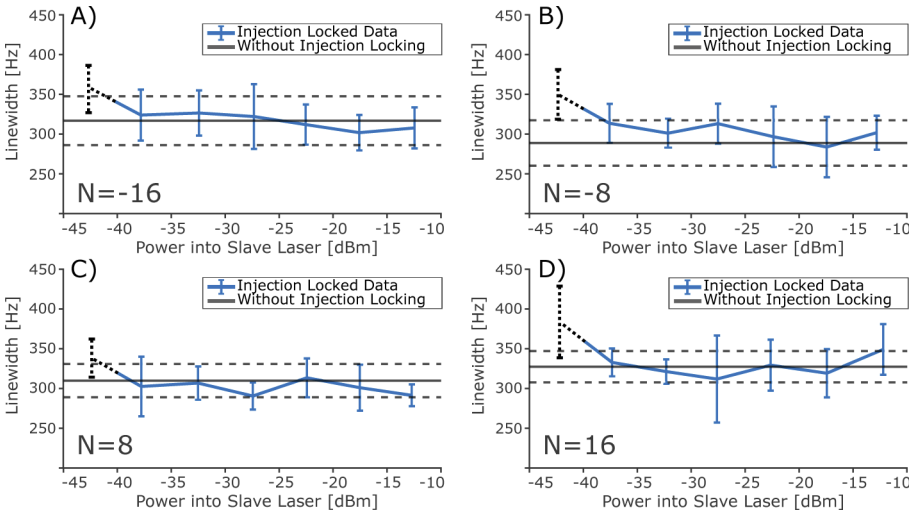

Fig. 6. Linewidth versus input power curves for A) $N = -16$, B) $N = -8$, C) $N = 8$, and D) $N = 16$ comb indices. In all cases, 15 measurements are taken at each frequency, and the error bars represent the standard deviation of these measurements. Here, the dark grey horizontal lines represent the unlocked linewidth, and the horizontal dashed lines represent the error bars of the unlocked linewidth. The dashed black lines indicate the region of unstable OIL.

Optics EXPRESS

To complete the investigation into the limits of injection locking, the $N = 0$ tone is selected from the comb using a POF, incrementally attenuated, and subsequently amplified up to −30 dBm using an EDFA. The tone is then used as the master for OIL, and the injection locked tone's linewidth is measured. The resulting plot of input OSNR vs measured linewidth is seen in Fig. 7. Stable optical injection with no observable penalty in linewidth requires approximately 30 dB of OSNR for a fixed input power of −30 dBm [39], at which point the ASE acquired during pre-amplification contributes to the injection locking of the DFB and corrupts the measured linewidth. Even a significant decrease in input OSNR (down to 20 dB) only produces a small increase in measured linewidth, on the order of a few hundred Hz. The use of an additional EDFA in our system therefore permits injection locking with no discernible penalty in linewidth of approximately 6 additional tones, which corresponds to an additional 150 GHz of black-box output tunablity.

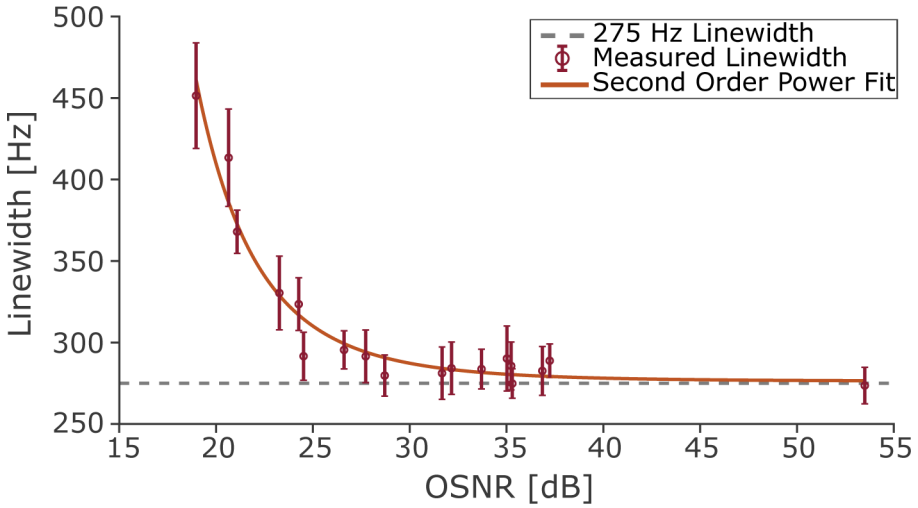

Fig. 7. The measured linewidth of the slave laser as a function of injected OSNR after attenuation and subsequent amplification, as measured on an OSA with 0.1 nm bandwidth, after filtration, at a central pump frequency of 192.9 THz. Here, 10 measurements are taken at each frequency, and the error bars represent the standard deviation of these measurements. All measurements are taken well outside of the power-limited regime, and all optical spectra were nearly identical to those pictured above.

4. Conclusion and future outlook

In conclusion, we have demonstrated a highly-tunable (~ 1.25 THz), high power (~100 mW), high side band suppression ratio (> 55 dB), and low linewidth (< 400 Hz) single frequency laser via the creation of an EO comb, selection of individual comb teeth via a POF, and subsequent optical injection locking of these tones using a set of three DFB slave lasers.

Assuming a 25 GHz comb created using the RF synthesizer as above and a pump at the center of the C-Band (193.725 THz, or 1547.5 nm) whose linewidth is approximately 275 Hz, the full C-Band could be reached with less than 750 Hz of linewidth across its range. Alternatively, the full C-Band could be reached with less than 1.5 kHz of linewidth across its full range using a commercial VCO.

However, in our case the EO comb spectra fails to cover the full C-Band. In the future, this problem may be remedied by up-scaling the system via the insertion of additional phase modulators before the amplitude modulator during the process of comb-creation, via non-linear

Optics EXPRESS

broadening of the comb in HNLF or photonic waveguides, or the use of multiple frequency combs / source lasers (which may serve to even further reduce the highest observed linewidth in such a system). Alternatively, it has been shown that stable injection locking down to −70 dBm is possible with the use of phase-locked loops [40], although it should be noted that this adds significant complexity to the system.

Finally, there may be interest in seeding the EO comb using a source which is even more tunable or even lower in linewidth than the fiber laser used here, in increasing the modulation frequency and thus FSR of the comb, in using a comb source other than an electro-optic comb such as a dark soliton comb [41,42], or in replacing the DFB slave laser array with a single Fabry-Perot type slave laser. All solutions may provide various benefits or drawbacks in terms of achievable bandwidth, linewidth, price, complexity, and size. This work represents a first step in the exploration of this parameter space, and an description the general approach.

Funding. Knut och Alice Wallenbergs Stiftelse; Vetenskapsrådet (VR-2015-00535).

Disclosures. The authors declare no conflicts of interest.

Data availability. Data underlying the results presented in this paper are not publicly available at this time but may be obtained from the authors upon reasonable request.

References

1. S. Fu, W. Shi, Y. Feng, L. Zhang, Z. Yang, S. Xu, X. Zhu, R. A. Norwood, and N. Peyghambarian, "Review of recent progress on single-frequency fiber lasers," J. Opt. Soc. Am. B **34**(3), A49–A62 (2017).
2. N. R. Newbury and W. C. Swann, "Low-noise fiber-laser frequency combs," J. Opt. Soc. Am. B **24**(8), 1756–1770 (2007).
3. H. Margolis, "Frequency metrology and clocks," J. Phys. B: At., Mol. Opt. Phys. **42**(15), 154017 (2009).
4. M. G. Hansen, E. Magoulakis, Q.-F. Chen, I. Ernsting, and S. Schiller, "Quantum cascade laser-based mid-IR frequency metrology system with ultra-narrow linewidth and 1× 10-13-level frequency instability," Opt. Lett. **40**(10), 2289–2292 (2015).
5. B. Lu, F. Wei, Z. Zhang, D. Xu, Z. Pan, D. Chen, and H. Cai, "Research on tunable local laser used in ground-to-satellite coherent laser communication," Chin. Opt. Lett. **13**(9), 091402–091406 (2015).
6. B. Stern, X. Ji, A. Dutt, and M. Lipson, "Compact narrow-linewidth integrated laser based on a low-loss silicon nitride ring resonator," Opt. Lett. **42**(21), 4541–4544 (2017).
7. M. Qiu, Q. Zhuge, M. Chagnon, F. Zhang, and D. V. Plant, "Laser phase noise effects and joint carrier phase recovery in coherent optical transmissions with digital subcarrier multiplexing," IEEE Photonics J. **9**(1), 1–13 (2017).
8. D. Pilori, A. Nespola, F. Forghieri, and G. Bosco, "Non-linear phase noise mitigation over systems using constellation shaping," J. Lightwave Technol. **37**(14), 3475–3482 (2019).
9. S. Gomez, H. Huang, J. Duan, B. Sawadogo, A. Gallet, A. Shen, S. Combrié, G. Baili, A. de Rossi, and F. Grillot, "10 Gbps error-free transmission of a high coherent si/iii-v hybrid distributed feedback laser under strong optical feedback," in *2019 IEEE Photonics Conference (IPC)*, (IEEE, 2019), pp. 1–2.
10. M. Norcia, A. Young, and A. Kaufman, "Microscopic control and detection of ultracold strontium in optical-tweezer arrays," Phys. Rev. X **8**(4), 041054 (2018).
11. R. X. Adhikari, "Gravitational radiation detection with laser interferometry," Rev. Mod. Phys. **86**(1), 121–151 (2014).
12. J. Duan, H. Huang, Z. Lu, P. Poole, C. Wang, and F. Grillot, "Narrow spectral linewidth in InAs/InP quantum dot distributed feedback lasers," Appl. Phys. Lett. **112**(12), 121102 (2018).
13. E. Di Gaetano, S. Watson, E. McBrearty, M. Sorel, and D. Paul, "Sub-megahertz linewidth 780.24 nm distributed feedback laser for 87 Rb applications," Opt. Lett. **45**(13), 3529–3532 (2020).
14. J. Xu, J. Ye, H. Xiao, J. Leng, J. Wu, H. Zhang, and P. Zhou, "Narrow-linewidth Q-switched random distributed feedback fiber laser," Opt. Express **24**(17), 19203–19210 (2016).
15. A. Becker, V. Sichkovskyi, M. Bjelica, O. Eyal, P. Baum, A. Rippien, F. Schnabel, B. Witzigmann, G. Eisenstein, and J. P. Reithmaier, "Narrow-linewidth 1.5-μm quantum dot distributed feedback lasers," in *Novel In-Plane Semiconductor Lasers XV*, vol. 9767 (International Society for Optics and Photonics, 2016), p. 97670Q.
16. J. W. Zimmerman, R. K. Price, U. Reddy, N. L. Dias, and J. J. Coleman, "Narrow linewidth surface-etched DBR lasers: Fundamental design aspects and applications," IEEE J. Sel. Top. Quantum Electron. **19**(4), 1503712 (2013).
17. M. Yamoah, B. Braverman, E. Pedrozo-Peñafiel, A. Kawasaki, B. Zlatković, and V. Vuletić, "Robust kHz-linewidth distributed Bragg reflector laser with optoelectronic feedback," Opt. Express **27**(26), 37714–37720 (2019).
18. C. Xiang, P. A. Morton, and J. E. Bowers, "Ultra-narrow linewidth laser based on a semiconductor gain chip and extended SiN Bragg grating," Opt. Lett. **44**(15), 3825–3828 (2019).
19. D. Huang, M. A. Tran, J. Guo, J. Peters, T. Komljenovic, A. Malik, P. A. Morton, and J. E. Bowers, "High-power sub-kHz linewidth lasers fully integrated on silicon," Optica **6**(6), 745–752 (2019).

Optics EXPRESS

20. H. Virtanen, A. T. Aho, J. Viheriälä, V.-M. Korpijärvi, T. Uusitalo, M. Koskinen, M. Dumitrescu, and M. Guina, "Spectral characteristics of narrow-linewidth high-power 1180 nm DBR laser with surface gratings," IEEE Photonics Technol. Lett. **29**(1), 114–117 (2017).
21. W. Shi, Q. Fang, X. Zhu, R. A. Norwood, and N. Peyghambarian, "Fiber lasers and their applications," Appl. Opt. **53**(28), 6554–6568 (2014).
22. Y. Zhang, Y. Zhang, Q. Zhao, C. Li, C. Yang, Z. Feng, H. Deng, E. Zhou, X. Xu, K. K. Wong, Z. Yang, and S. Xu, "Ultra-narrow linewidth full c-band tunable single-frequency linear-polarization fiber laser," Opt. Express **24**(23), 26209–26214 (2016).
23. Z. Wu, Q. Zhao, C. Yang, K. Zhou, W. Lin, X. Guan, C. Li, T. Tan, Z. Feng, Z. Yang, and S. Xu, "Simultaneously improving the linewidth and the low-frequency relative intensity noise of a single-frequency fiber laser," Appl. Phys. Express **12**(5), 052018 (2019).
24. W. Ji, S. Chen, L. Fu, and Z. Zou, "Experimental study of an ultra narrow linewidth fiber laser by injection locking," Chin. Opt. Lett. **10**(8), 080601 (2012).
25. S. Li, N. Ngo, and Z. Zhang, "Tunable fiber laser with ultra-narrow linewidth using a tunable phase-shifted chirped fiber grating," IEEE Photonics Technol. Lett. **20**(17), 1482–1484 (2008).
26. H. Al-Taiy, N. Wenzel, S. Preußler, J. Klinger, and T. Schneider, "Ultra-narrow linewidth, stable and tunable laser source for optical communication systems and spectroscopy," Opt. Lett. **39**(20), 5826–5829 (2014).
27. A. Parriaux, K. Hammani, and G. Millot, "Electro-optic frequency combs," Adv. Opt. Photonics **12**(1), 223–287 (2020).
28. Z. Tong, A. O. Wiberg, E. Myslivets, B. P. Kuo, N. Alic, and S. Radic, "Spectral linewidth preservation in parametric frequency combs seeded by dual pumps," Opt. Express **20**(16), 17610–17619 (2012).
29. R. Slavik, F. Parmigiani, L. Gruner-Nielsen, D. Jakobsen, S. Herstrom, P. Petropoulos, and D. Richardson, "Stable and efficient generation of high repetition rate (>160 GHz) subpicosecond optical pulses," IEEE Photonics Technol. Lett. **23**(9), 540–542 (2011).
30. A. Ishizawa, T. Nishikawa, K. Hitachi, K. Hitomi, and H. Gotoh, "Ultra-low phase noise microwave generation with 25-Ghz electro-optics-modulation comb," in *2019 24th OptoElectronics and Communications Conference (OECC) and 2019 International Conference on Photonics in Switching and Computing (PSC)*, (IEEE, 2019), pp. 1–3.
31. A. Ishizawa, T. Nishikawa, A. Mizutori, H. Takara, A. Takada, T. Sogawa, and M. Koga, "Phase-noise characteristics of a 25-GHz-spaced optical frequency comb based on a phase-and intensity-modulated laser," Opt. Express **21**(24), 29186–29194 (2013).
32. S. Hisatake, Y. Nakase, K. Shibuya, and T. Kobayashi, "Generation of flat power-envelope terahertz-wide modulation sidebands from a continuous-wave laser based on an external electro-optic phase modulator," Opt. Lett. **30**(7), 777–779 (2005).
33. Z. Wang, C. Ke, Y. Zhong, C. Xing, H. Wang, K. Yang, S. Cui, and D. Liu, "Ultra-narrow-linewidth measurement utilizing dual-parameter acquisition through a partially coherent light interference," Opt. Express **28**(6), 8484–8493 (2020).
34. S. Huang, T. Zhu, Z. Cao, M. Liu, M. Deng, J. Liu, and X. Li, "Laser linewidth measurement based on amplitude difference comparison of coherent envelope," IEEE Photonics Technol. Lett. **28**(7), 759–762 (2016).
35. Z. Liu and R. Slavík, "Optical injection locking: From principle to applications," J. Lightwave Technol. **38**(1), 43–59 (2020).
36. A. Murakami, K. Kawashima, and K. Atsuki, "Cavity resonance shift and bandwidth enhancement in semiconductor lasers with strong light injection," IEEE J. Quantum Electron. **39**(10), 1196–1204 (2003).
37. F. Mogensen, H. Olesen, and G. Jacobsen, "Locking conditions and stability properties for a semiconductor laser with external light injection," IEEE J. Quantum Electron. **21**(7), 784–793 (1985).
38. A. Bordonalli, C. Walton, and A. J. Seeds, "High-performance phase locking of wide linewidth semiconductor lasers by combined use of optical injection locking and optical phase-lock loop," J. Lightwave Technol. **17**(2), 328–342 (1999).
39. M. Ruiz Garcia, "Effects of ASE noise and total injected power on optical injection locking," Master's thesis, Chalmers University of Technology, 2019.
40. R. Kakarla, J. Schröder, and P. A. Andrekson, "Optical injection locking at sub nano-watt powers," Opt. Lett. **43**(23), 5769–5772 (2018).
41. X. Xue, Y. Xuan, Y. Liu, P.-H. Wang, S. Chen, J. Wang, D. E. Leaird, M. Qi, and A. M. Weiner, "Mode-locked dark pulse Kerr combs in normal-dispersion microresonators," Nat. Photonics **9**(9), 594–600 (2015).
42. Ó. B. Helgason, F. R. Arteaga-Sierra, Z. Ye, K. Twayana, P. A. Andrekson, M. Karlsson, J. Schröder, and V. Torres-Company, "Dissipative solitons in photonic molecules," Nat. Photonics **15**(4), 305–310 (2021).